

Analytical Computation of g-Factor Maps for Autocalibrated Parallel Imaging

P. J. Beatty¹, and A. C. Brau¹

¹MR Applied Science Lab, GE Healthcare, Menlo Park, CA, United States

The g-factor map [1] is a useful way to visualize the increase in noise due to parallel imaging reconstruction. Robson et al. have shown a general approach for computing g-factor maps that repeatedly injects a small amount of noise into the data and reconstructs the image [2]. Still, it is useful to have analytical approaches that directly calculate the g-factor map, where possible. It has been shown that g-factor maps can be created for GRAPPA reconstructions when the calibration phase encodes (ACS lines) are not included as data for the final image, allowing the reconstruction coefficients to be converted into the image domain [3,4]. When the ACS lines are included in the final reconstruction, forming a g-factor map for this variable density trajectory becomes more difficult because the operation of filling in missing data can no longer be treated strictly as a convolution in k-space.

In this work, we describe how g-factor maps can be computed directly from the unaliasing coefficients used in autocalibrated parallel imaging. The proposed method is implemented and results are shown demonstrating the usefulness of g-factor maps in two important areas pertaining to autocalibrated parallel imaging: coil combination and reconstruction kernel size. In this study, we focus on variable density Cartesian acquisitions, however the proposed method can also be used to analytically compute g-factor maps for non-Cartesian parallel imaging methods that use local k-space kernels [5-10].

Theory Image space noise covariance maps for separate coil images can be computed from the noise covariance between k-space locations, as shown in Fig. 1a. While there is no noise covariance between different k-space locations in unaccelerated scans, the unaliasing coefficients in autocalibrated parallel imaging create noise covariance between k-space locations as well as between channels (Fig 1b). Due to the limited k-space extent of unaliasing kernels, image space noise covariance maps can be efficiently computed directly from the unaliasing coefficients [11]. Separate coil images are typically combined using square-root sum-of-squares (SOS), a non-linear operation. However, as illustrated in Fig. 2, this operation can be accurately approximated as a linear operation at image locations possessing sufficient signal. This linear approximation allows the g-factor map for the combined image to be computed.

Methods A fat/water phantom was scanned at 1.5T (Signa® HDx, GE Healthcare, Waukesha, WI) using an 8-channel body array. An outer acceleration factor of two was used with 12 additional calibration phase encodes. The data was reconstructed using 3x3 and 7x7 unaliasing kernels, with coil image combination performed by SOS and by linear combination [12], using the low-resolution calibration data to estimate relative coil sensitivities. Analytical computation of g-

factor maps for autocalibrated parallel imaging was implemented and used to compute g-factor maps for each reconstruction. The reconstructed images and g-factor maps were used to study the image quality differences attributable to the choice of kernel size and coil combination method.

Results and Discussion Results are shown in Fig. 3. The analytically computed g-factor maps correctly identified the image regions of increased noise amplification. The computed g-factor maps indicate that linear combination of the separate coil images, using low resolution coil sensitivity estimates, results in a similar signal-to-noise ratio as SOS combination. While SOS combination cannot be used with phase-sensitive applications, these applications can use linear combination, since a complex-valued combined image is generated, without incurring any additional SNR penalty from coil combination. The choice of unaliasing kernel size is still a challenging task for autocalibrated parallel imaging and this choice can appreciably impact image quality, as seen in Fig. 3. Since a g-factor map can be computed for each potential kernel choice, even before the image is reconstructed, g-factor maps can aid in automatic kernel size selection. g-Factor maps provide an intuitive way to assess the noise penalty associated with different reconstruction parameter choices; the computationally efficient analytical method for g-factor map generation proposed in this work can make it easier to take advantage of g-factor maps.

References [1] Pruessmann et al. MRM 1999 42:952-62. [2] Robson et al. ISMRM 2007, p1747. [3] Griswold, Sec. Int. Workshop on Parallel MRI, 2004. [4] Wang et al. ISMRM 2005, p2428. [5] Yeh et al. MRM 2005 53:1383-92. [6] Griswold et al. ISMRM 2003, p2349. [7] Heberlein et al. MRM 2006 55:619-25. [8] Heidemann et al. Sec. Int. Workshop on Parallel MRI, 2004. [9] Seiberlich et al., ISMRM 2007, p334. [10] Beatty et al., ISMRM 2007, p335. [11] Beatty, Ph.D. diss., Stanford, 2006. [12] Roemer et al., MRM 1990 16:192-225.

(a)
$$\text{VAR}(\mathbf{r}) = \sum_{\mathbf{k}_1} \sum_{\mathbf{k}_2} \Psi_{\mathbf{k}_1, \mathbf{k}_2} e^{i2\pi(\mathbf{k}_2 - \mathbf{k}_1) \cdot \mathbf{r}}$$

(b)
$$\Psi_{\mathbf{k}_1, \mathbf{k}_2} = \mathbf{W}_{12} \sigma^2$$

● acquired location \mathbf{k}_1
○ synthesized location \mathbf{k}_2

\mathbf{W}_{12} \mathbf{W}_{32}

Figure 1: (a) Equation for computing the noise variance at image location \mathbf{r} as a function of noise covariance (Ψ) between k-space locations \mathbf{k}_1 and \mathbf{k}_2 . (b) Without parallel imaging, the noise at each k-space location is independent. With parallel imaging, the noise covariance can be related to the unaliasing coefficients, \mathbf{w} .

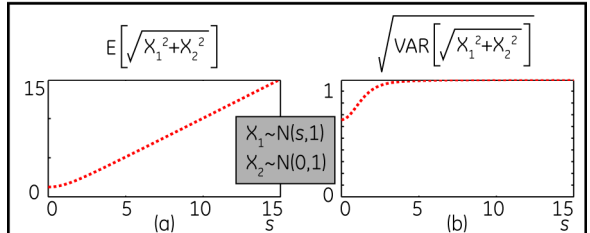


Figure 2: Justification for linear approximation of square-root sum-of-squares (SOS) non-linear operation. Consider the SOS of two Gaussian random variables, X_1 and X_2 . X_1 has mean signal s and X_2 has zero mean; both have unit variance. Plotted is (a) mean and (b) variance versus mean signal s of the resultant random variable. As can be seen, approximating this random variable as Gaussian with mean s and unit variance is very accurate for $s > 5$, corresponding to an SNR greater than 5, which is adequate for most situations in MR.

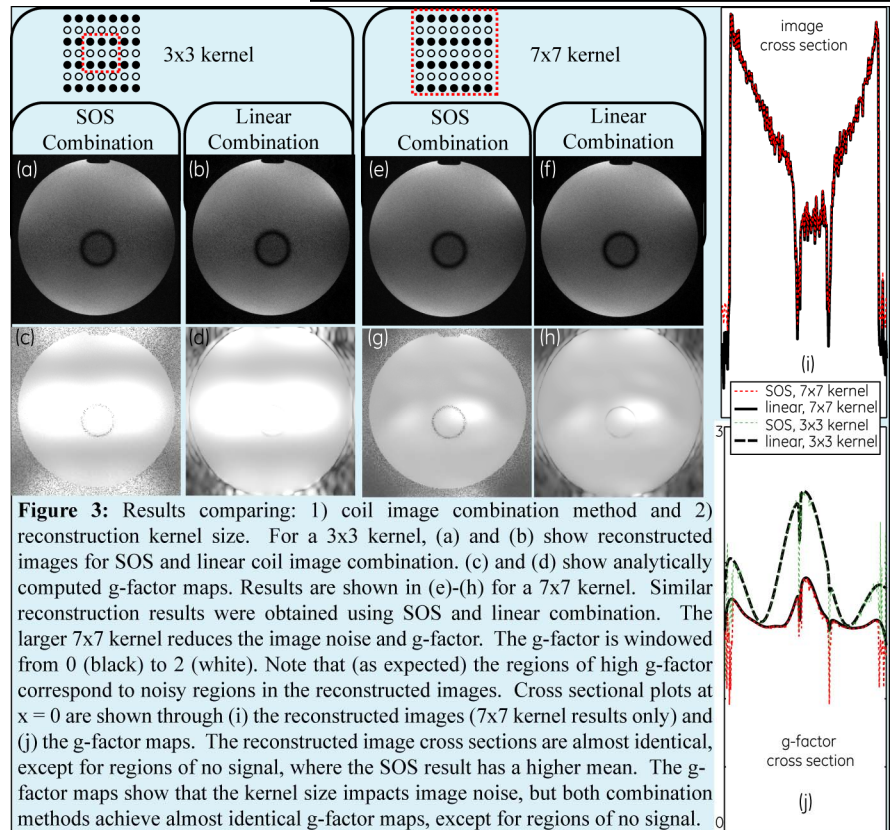


Figure 3: Results comparing: 1) coil image combination method and 2) reconstruction kernel size. For a 3x3 kernel, (a) and (b) show reconstructed images for SOS and linear coil image combination. (c) and (d) show analytically computed g-factor maps. Results are shown in (e)-(h) for a 7x7 kernel. Similar reconstruction results were obtained using SOS and linear combination. The larger 7x7 kernel reduces the image noise and g-factor. The g-factor is windowed from 0 (black) to 2 (white). Note that (as expected) the regions of high g-factor correspond to noisy regions in the reconstructed images. Cross sectional plots at $x = 0$ are shown through (i) the reconstructed images (7x7 kernel results only) and (j) the g-factor maps. The reconstructed image cross sections are almost identical, except for regions of no signal, where the SOS result has a higher mean. The g-factor maps show that the kernel size impacts image noise, but both combination methods achieve almost identical g-factor maps, except for regions of no signal.